LEIBNIZ-INFORMATIONSZENTRUM
TECHNIK UND NATURWISSENSCHAFTEN
UNIVERSITÄTSBIBLIOTHEK

TIB

FAIR scientific information with the Open Research Knowledge Graph

Markus Stocker
December 13, 2022
e-IRG Workshop

Leibniz Gemeinschaft

failure than in LV tissue samples from unused donor hearts (*Figure 1A*). As shown by electrophoretic mobility shift assays, IRE binding activity was significantly reduced in failing hearts (most pronounced in patients with ischemic cardiomyopathy) (*Figure 1B*). Protein expression levels of the transferrin receptor were significantly lower in failing hearts than in the controls (*Figure 1C*).

Targeted Irp deletion in mice induces ID in the myocardium

We generated mice with a cardiomyocyte-targeted deletion of *Irp1* and *Irp2* (Cre-Irp1/2$^{0/0}$) to address Irp function in the heart (*Figure 2A*). Cre-Irp1/2$^{0/0}$ mice were born at the expected Mendelian inheritance ratio and survived into adulthood. Reverse transcriptase polymerase chain reaction on LV myocardium and isolated cardiomyocytes demonstrated near-complete Cre-mediated deletion of Irp1 and Irp2 mRNAs in cardiomyocytes from Cre-Irp1/2$^{f/f}$ mice compared with littermates lacking the Cre transgene (Irp1/2$^{f/f}$) (*Figure 2B*). Irp1 and Irp2 protein expression was markedly reduced in LV myocardium and barely detectable in isolated cardiomyocytes from Cre-Irp1/2$^{0/0}$ mice (*Figure 2C and D*). Irp1 and Irp2 protein expression in the liver was similar in Cre-Irp1/2$^{f/f}$ and Irp1/2$^{f/f}$ mice (*Figure 2C* and *D*). IRE binding activity was strongly reduced in isolated cardiomyocytes from Cre-Irp1/2$^{0/0}$ mice (*Figure 2E*), confirming near-complete Cre-mediated recombination. Iron-regulatory protein/IRE-regulated proteins involved in iron transport and storage were differentially regulated in cardiomyocytes from Cre-Irp1/2$^{0/0}$ mice: the transferrin receptor was down-regulated (25 ± 14% of Irp1/2$^{f/f}$ controls, $P = 0.006$), whereas ferroportin (325 ± 9%, $P = 0.003$) and ferritin H-chain (249 ± 35%, $P = 0.012$) were up-regulated ($n = 3$ per group; representative immunoblots are presented in *Figure 2F*). As a result, iron concentration in cardiomyocytes was significantly reduced in Cre-Irp1/2$^{0/0}$ mice (*Figure 2G*). Likewise, iron concentration in the left ventricle was reduced in Cre-Irp1/2$^{0/0}$ mice compared with Irp1/2$^{0/0}$ controls, whereas iron concentrations in the M. quadriceps femoris and liver were not affected (*Figure 2H*). Iron concentration in the left ventricle was normal in Cre mice showing that cardiac ID in Cre-Irp1/2$^{0/0}$ mice was not related to Cre transgene expression per se (*Figure 2H*). Haem and myoglobin concentrations were significantly reduced in the left ventricle of Cre-Irp1/2$^{0/0}$ mice (*Figure 2I* and *J*). Copper and free radical concentrations in the left ventricle were similar in Cre-Irp1/2$^{f/f}$ and Irp1/2$^{0/0}$ mice (see Supplementary material online, *Figure S2*).

Cre-Irp1/2$^{0/0}$ mice did not show an obvious phenotype under baseline conditions. Body mass, heart mass, LV mass, and cardiomyocyte cross-sectional area were similar in Cre-Irp1/2$^{0/0}$ and Irp1/2$^{0/0}$ mice under baseline conditions (see Supplementary material online, *Table S1*). On echocardiography, LV end-diastolic and end-systolic dimensions and LV systolic and diastolic function were similar in both genotypes (see Supplementary material online, *Table S1*). Cre-Irp1/2$^{0/0}$ mice were not anaemic and had a normal peripheral blood count (see Supplementary material online, *Table S2*).

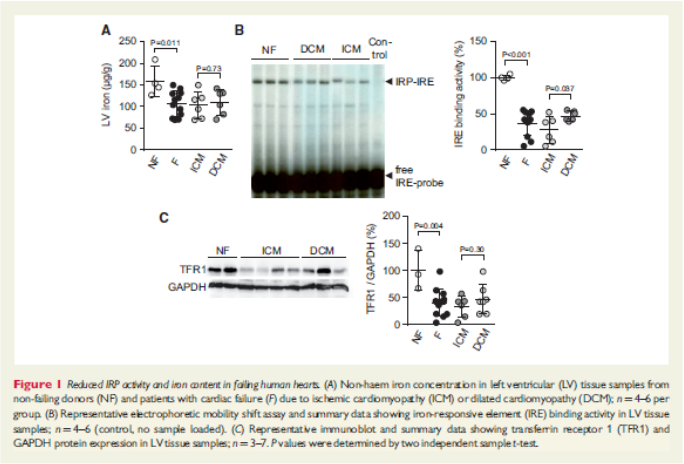

Figure 1 *Reduced IRP activity and iron content in failing human hearts.* (A) Non-haem iron concentration in left ventricular (LV) tissue samples from non-failing donors (NF) and patients with cardiac failure (*F*) due to ischemic cardiomyopathy (ICM) or dilated cardiomyopathy (DCM); $n = 4$–6 per group. (B) Representative electrophoretic mobility shift assay and summary data showing iron-responsive element (IRE) binding activity in LV tissue samples; $n = 4$–6 (control, no sample loaded). (C) Representative immunoblot and summary data showing transferrin receptor 1 (TFR1) and GAPDH protein expression in LV tissue samples; $n = 3$–7. *P* values were determined by two independent sample *t*-test.

https://doi.org/10.1093/eurheartj/ehw333

Scientific information is data
This data is not FAIR
Certainly not for machines

We find and access documents

failure than in LV tissue samples from unused donor hearts (*Figure 1A*). As shown by electrophoretic mobility shift assays, IRE binding activity was significantly reduced in failing hearts (most pronounced in patients with ischemic cardiomyopathy) (*Figure 1B*). Protein expression levels of the transferrin receptor were significantly lower in failing hearts than in the controls (*Figure 1C*).

Targeted Irp deletion in mice induces ID in the myocardium

We generated mice with a cardiomyocyte-targeted deletion of *Irp1* and *Irp2* (Cre-Irp1/2^{0f}) to address Irp function in the heart (*Figure 2A*). Cre-Irp1/2^{0f} mice were born at the expected Mendelian inheritance ratio and survived into adulthood. Reverse transcriptase polymerase chain reaction on LV myocardium and isolated cardiomyocytes demonstrated near-complete Cre-mediated deletion of Irp1 and Irp2 mRNAs in cardiomyocytes from Cre-Irp1/2$^{f/f}$ mice compared with littermates lacking the Cre transgene (Irp1/2^{0f}) (*Figure 2B*). Irp1 and Irp2 protein expression was markedly reduced in LV myocardium and barely detectable in isolated cardiomyocytes from Cre-Irp1/2^{0f} mice (*Figure 2C and D*). Irp1 and Irp2 protein expression in the liver was similar in Cre-Irp1/2$^{f/f}$ and Irp1/2$^{f/f}$ mice (*Figure 2C* and *D*). IRE binding activity was strongly reduced in isolated cardiomyocytes from Cre-Irp1/2^{0f} mice (*Figure 2E*), confirming near-complete Cre-mediated recombination. Iron-regulatory protein/IRE-regulated proteins involved in iron transport and storage were differentially regulated in cardi

per group; represent
2F). As a result, iron con
cantly reduced in Cre-I
concentration in the lef
mice compared with Irp
tions in the M. quadrice
(*Figure 2H*). Iron concent
Cre mice showing that
related to Cre transgen
and myoglobin concentr
left ventricle of Cre-Irp1/2
free radical concentrations in the left ventricle were similar in Cre-Irp1/2$^{f/f}$ and Irp1/2^{0f} mice (see Supplementary material online, *Figure S2*).

Cre-Irp1/2^{0f} mice did not show an obvious phenotype under baseline conditions. Body mass, heart mass, LV mass, and cardiomyocyte cross-sectional area were similar in Cre-Irp1/2^{0f} and Irp1/2^{0f} mice under baseline conditions (see Supplementary material online, *Table S1*). On echocardiography, LV end-diastolic and end-systolic dimensions and LV systolic and diastolic function were similar in both genotypes (see Supplementary material online, *Table S1*). Cre-Irp1/2^{0f} mice were not anaemic and had a normal peripheral blood count (see Supplementary material online, *Table S2*).

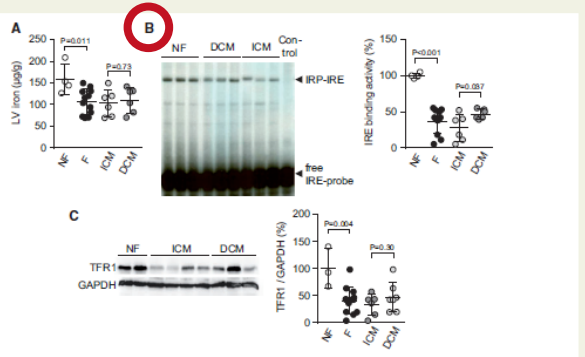

Figure 1 *Reduced IRP activity and iron content in failing human hearts.* (A) Non-haem iron concentration in left ventricular (LV) tissue samples from non-failing donors (NF) and patients with cardiac failure (*F*) due to ischemic cardiomyopathy (ICM) or dilated cardiomyopathy (DCM); $n = 4$–6 per group. (B) Representative electrophoretic mobility shift assay and summary data showing iron-responsive element (IRE) binding activity in LV tissue samples; $n = 4$–6 (control, no sample loaded). (C) Representative immunoblot and summary data showing transferrin receptor 1 (TFR1) and GAPDH protein expression in LV tissue samples; $n = 3$–7. *P* values were determined by two independent sample *t*-test.

https://doi.org/10.1093/eurheartj/ehw333

failure than in LV tissue samples from unused donor hearts (*Figure 1A*). As shown by electrophoretic mobility shift assays, IRE binding activity was significantly reduced in failing hearts (most pronounced in patients with ischemic cardiomyopathy) (*Figure 1B*). Protein expression levels of the transferrin receptor were significantly lower in failing hearts than in the controls (*Figure 1C*).

Targeted Irp deletion in mice induces ID in the myocardium

We generated mice with a cardiomyocyte-targeted deletion of *Irp1* and *Irp2* (Cre-Irp1/2$^{0/f}$) to address Irp function in the heart (*Figure 2A*). Cre-Irp1/2$^{0/f}$ mice were born at the expected Mendelian inheritance ratio and survived into adulthood. Reverse transcriptase polymerase chain reaction on LV myocardium and isolated cardiomyocytes demonstrated near-complete Cre-mediated deletion of Irp1 and Irp2 mRNAs in cardiomyocytes from Cre-Irp1/2$^{f/f}$ mice compared with littermates lacking the Cre transgene (Irp1/2$^{f/f}$) (*Figure 2B*). Irp1 and Irp2 protein expression was markedly reduced in LV myocardium and barely detectable in isolated cardiomyocytes from Cre-Irp1/2$^{0/f}$ mice (*Figure 2C and D*). Irp1 and Irp2 protein expression in the liver was similar in Cre-Irp1/2$^{f/f}$ and Irp1/2$^{f/f}$ mice (*Figure 2C and D*). IRE binding activity was strongly reduced in isolated cardiomyocytes from Cre-Irp1/2$^{0/f}$ mice (*Figure 2E*), confirming near-complete Cre-mediated recombination. Iron-regulatory protein/IRE-regulated proteins involved in iron transport and storage were differentially regulated in cardi

per group; represent
2F). As a result, iron con
cantly reduced in Cre-I
concentration in the lef
mice compared with Irp
tions in the M. quadrice
(*Figure 2H*). Iron concent
Cre mice showing that
related to Cre transgen
and myoglobin concentr
left ventricle of Cre-Irp1/2
free radical concentrations in the left ventricle were similar in Cre-Irp1/2$^{f/f}$ and Irp1/2$^{0/f}$ mice (see Supplementary material online, *Figure S2*).

Cre-Irp1/2$^{0/f}$ mice did not show an obvious phenotype under baseline conditions. Body mass, heart mass, LV mass, and cardiomyocyte cross-sectional area were similar in Cre-Irp1/2$^{0/f}$ and Irp1/2$^{0/f}$ mice under baseline conditions (see Supplementary material online, *Table S1*). On echocardiography, LV end-diastolic and end-systolic dimensions and LV systolic and diastolic function were similar in both genotypes (see Supplementary material online, *Table S1*). Cre-Irp1/2$^{0/f}$ mice were not anaemic and had a normal peripheral blood count (see Supplementary material online, *Table S2*).

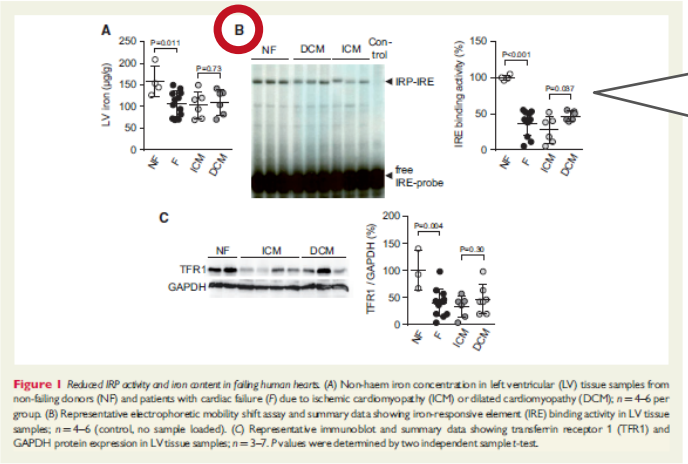

Figure 1 *Reduced IRP activity and iron content in failing human hearts.* (A) Non-haem iron concentration in left ventricular (LV) tissue samples from non-failing donors (NF) and patients with cardiac failure (*F*) due to ischemic cardiomyopathy (ICM) or dilated cardiomyopathy (DCM); $n = 4$–6 per group. (B) Representative electrophoretic mobility shift assay and summary data showing iron-responsive element (IRE) binding activity in LV tissue samples; $n = 4$–6 (control, no sample loaded). (C) Representative immunoblot and summary data showing transferrin receptor 1 (TFR1) and GAPDH protein expression in LV tissue samples; $n = 3$–7. *P* values were determined by two independent sample *t*-test.

CSV

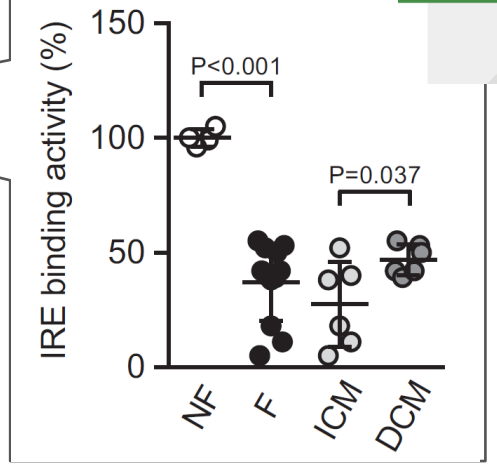

https://doi.org/10.1093/eurheartj/ehw333

failure than in LV tissue samples from unused donor hearts (*Figure 1A*). As shown by electrophoretic mobility shift assays, IRE binding activity was significantly reduced in failing hearts (most pronounced in patients with ischemic cardiomyopathy) (*Figure 1B*). Protein expression levels of the transferrin receptor were significantly lower in failing hearts than in the controls (*Figure 1C*).

Targeted Irp deletion in mice induces ID in the myocardium

We generated mice with a cardiomyocyte-targeted deletion of *Irp1* and *Irp2* (Cre-Irp1/2$^{0/f}$) to address Irp function in the heart (*Figure 2A*). Cre-Irp1/2$^{0/f}$ mice were born at the expected Mendelian inheritance ratio and survived into adulthood. Reverse transcriptase polymerase chain reaction on LV myocardium and isolated cardiomyocytes demonstrated near-complete Cre-mediated deletion of Irp1 and Irp2 mRNAs in cardiomyocytes from Cre-Irp1/2$^{f/f}$ mice compared with littermates lacking the Cre transgene (Irp1/2$^{f/f}$) (*Figure 2B*). Irp1 and Irp2 protein expression was markedly reduced in LV myocardium and barely detectable in isolated cardiomyocytes from Cre-Irp1/2$^{0/f}$ mice (*Figure 2C and D*). Irp1 and Irp2 protein expression in the liver was similar in Cre-Irp1/2$^{f/f}$ and Irp1/2$^{f/f}$ mice (*Figure 2C* and D). IRE binding activity was strongly reduced in isolated cardiomyocytes from Cre-Irp1/2$^{0/f}$ mice (*Figure 2E*), confirming near-complete Cre-mediated recombination. Iron-regulatory protein/IRE-regulated proteins involved in iron transport and storage were differentially regulated in cardi

per group; represent
2F). As a result, iron con
cantly reduced in Cre-I
concentration in the lef
mice compared with Irp
tions in the M. quadrice
(*Figure 2H*). Iron concent
Cre mice showing that
related to Cre transgen
and myoglobin concentr
left ventricle of Cre-Irp1/2
free radical concentrations in the left ventricle were similar in Cre-Irp1/2$^{f/f}$ and Irp1/2$^{0/f}$ mice (see Supplementary material online, *Figure S2*).

Cre-Irp1/2$^{0/f}$ mice did not show an obvious phenotype under baseline conditions. Body mass, heart mass, LV mass, and cardiomyocyte cross-sectional area were similar in Cre-Irp1/2$^{0/f}$ and Irp1/2$^{0/f}$ mice under baseline conditions (see Supplementary material online, *Table S1*). On echocardiography, LV end-diastolic and end-systolic dimensions and LV systolic and diastolic function were similar in both genotypes (see Supplementary material online, *Table S1*). Cre-Irp1/2$^{0/f}$ mice were not anaemic and had a normal peripheral blood count (see Supplementary material online, *Table S2*).

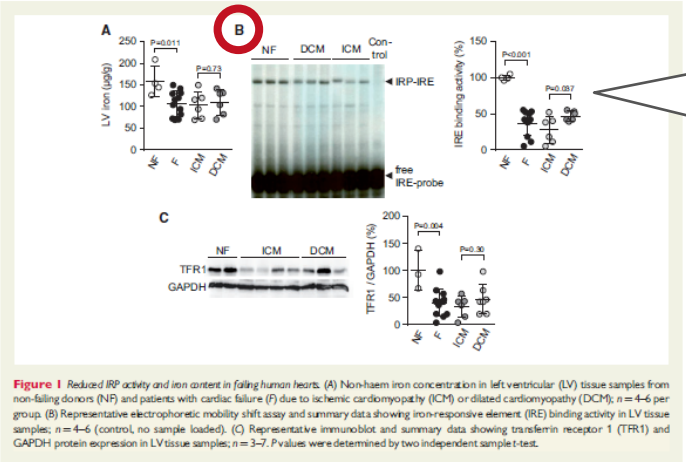

Figure 1 *Reduced IRP activity and iron content in failing human hearts.* (A) Non-haem iron concentration in left ventricular (LV) tissue samples from non-failing donors (NF) and patients with cardiac failure (*F*) due to ischemic cardiomyopathy (ICM) or dilated cardiomyopathy (DCM); $n = 4$–6 per group. (B) Representative electrophoretic mobility shift assay and summary data showing iron-responsive element (IRE) binding activity in LV tissue samples; $n = 4$–6 (control, no sample loaded). (C) Representative immunoblot and summary data showing transferrin receptor 1 (TFR1) and GAPDH protein expression in LV tissue samples; $n = 3$–7. *P* values were determined by two independent sample *t*-test.

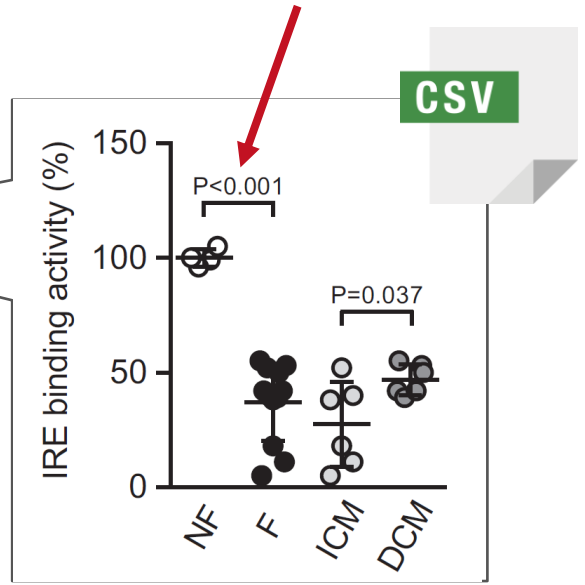

https://doi.org/10.1093/eurheartj/ehw333

This is what machines should consume

Student's t-test [http://purl.obolibrary.org/obo/OBI_0000739]

has dependent variable
iron-responsive element binding [http://amigo.geneontology.org/amigo/term/GO:0030350]

has specified input
https://doi.org/10.4563/zenodo.56980

has specified output
p-value [http://purl.obolibrary.org/obo/OBI_0000175]
scalar value specification "0.00000000131112475"^^xsd:decimal

https://doi.org/10.1093/eurheartj/ehw333

“Scientific writing can [...] be called *information burying*”

First we bury it and then we mine it again

-- Barend Mons (2005)

https://doi.org/10.1186/1471-2105-6-142

“we have failed to [...] organize [...] information [...] in rigorous [...] ways, so that finding what we want and understanding what's already known become [...] increasingly costly experiences”

-- Teresa K. Attwood et al. (2009)

https://doi.org/10.1042/BJ20091474

“Despite recent developments in machine learning [...], data extraction is still largely a manual process”

-- Julian Higgins et al. (2022)

https://training.cochrane.org/handbook/current

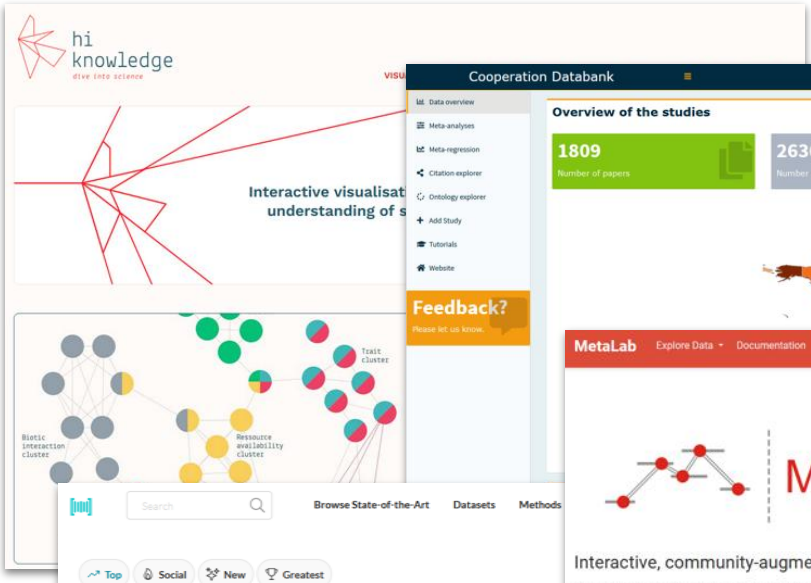
hi
knowledge
dive into science
Interactive visualisat
understanding of s
Trait
cluster
Biotic
interaction
cluster
Ressource
availability
cluster

Cooperation Databank
Data overview
Meta-analyses
Meta-regression
Citation explorer
Ontology explorer
Add Study
Tutorials
Website
Feedback?
Please let us know.
Overview of the studies
1809
Number of papers
2636
Number of studies
13934
Number of effects
Show studies by
Country/Region
Year of data collection
Sample size

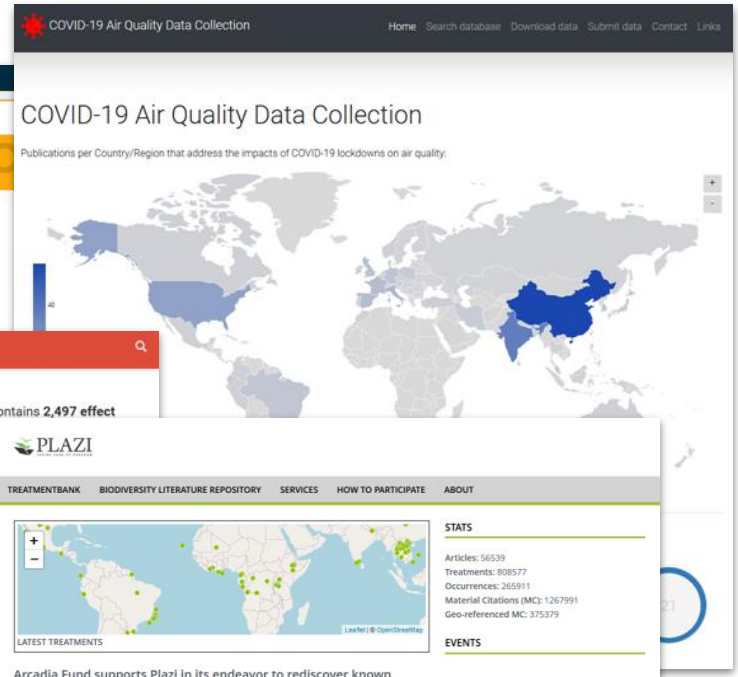
COVID-19 Air Quality Data Collection
Home
Search database
Download data
Submit data
Contact
Links
COVID-19 Air Quality Data Collection
Publications per Country/Region that address the impacts of COVID-19 lockdowns on air quality:

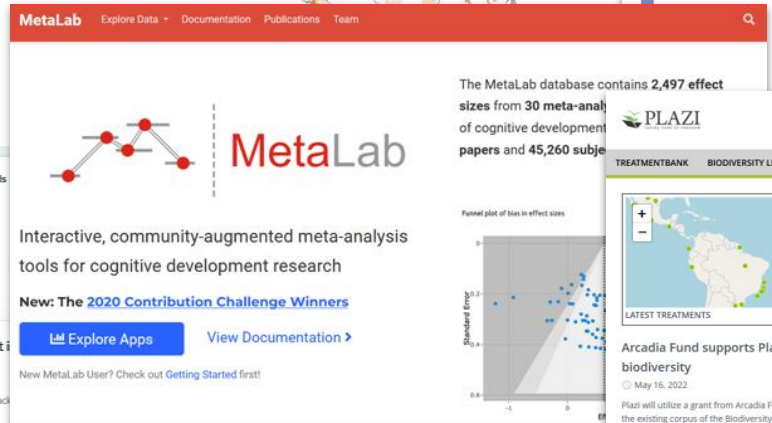
MetaLab
Explore Data
Documentation
Publications
Team
MetaLab
Interactive, community-augmented meta-analysis
tools for cognitive development research
New: The 2020 Contribution Challenge Winners
Explore Apps
View Documentation
New MetaLab User? Check out Getting Started first!
The MetaLab database contains 2,497 effect
sizes from 30 meta-anal
of cognitive development
papers and 45,260 subje
Funnel plot of bias in effect sizes
Standard Error
Domains
Early Language
How do children learn their native language?
Cognitive Devel
What is the nature of children

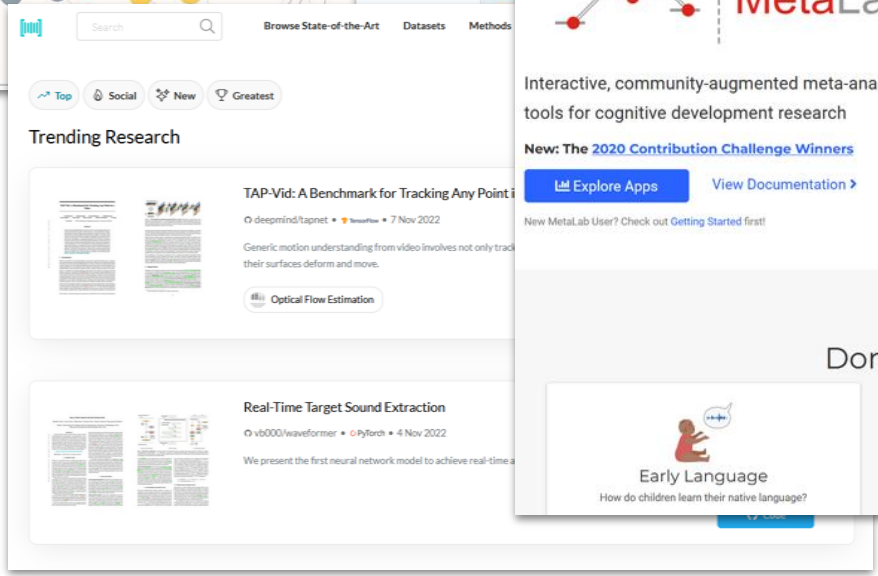
Search
Browse State-of-the-Art
Datasets
Methods
Top
Social
New
Greatest
Trending Research
TAP-Vid: A Benchmark for Tracking Any Point i
deepmind/tapnet
7 Nov 2022
Generic motion understanding from video involves not only track
their surfaces deform and move.
Optical Flow Estimation
Real-Time Target Sound Extraction
vb000/waveformer
PyTorch
4 Nov 2022
We present the first neural network model to achieve real-time a

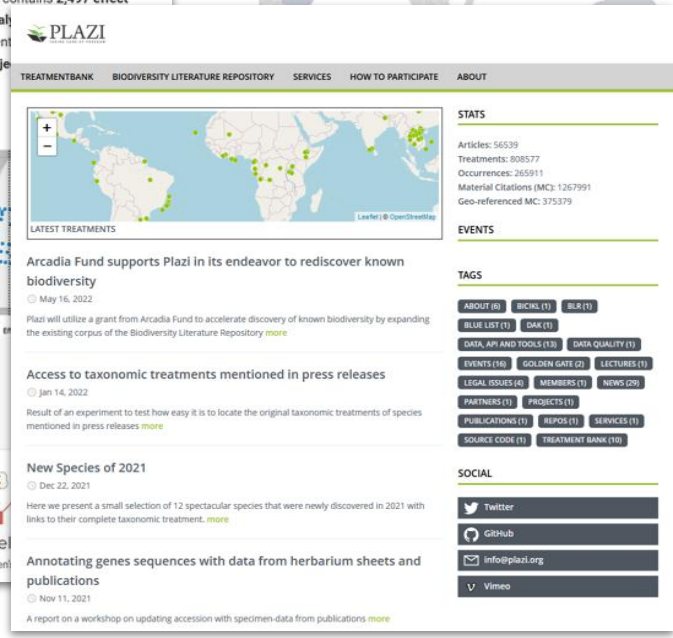
PLAZI
TREATMENTBANK
BIODIVERSITY LITERATURE REPOSITORY
SERVICES
HOW TO PARTICIPATE
ABOUT
LATEST TREATMENTS
STATS
Articles: 56539
Treatments: 808577
Occurrences: 265911
Material Citations (MC): 1267991
Geo-referenced MC: 375379
EVENTS
TAGS
ABOUT (6)
BICIKL (1)
BLR (1)
BLUE LIST (1)
DAK (1)
DATA, API AND TOOLS (13)
DATA QUALITY (1)
EVENTS (16)
GOLDEN GATE (2)
LECTURES (1)
LEGAL ISSUES (4)
MEMBERS (1)
NEWS (29)
PARTNERS (1)
PROJECTS (1)
PUBLICATIONS (1)
REPOS (1)
SERVICES (1)
SOURCE CODE (1)
TREATMENT BANK (10)
SOCIAL
Twitter
GitHub
info@plazi.org
Vimeo
Arcadia Fund supports Plazi in its endeavor to rediscover known biodiversity
May 16, 2022
Plazi will utilize a grant from Arcadia Fund to accelerate discovery of known biodiversity by expanding the existing corpus of the Biodiversity Literature Repository more
Access to taxonomic treatments mentioned in press releases
Jan 14, 2022
Result of an experiment to test how easy it is to locate the original taxonomic treatments of species mentioned in press releases more
New Species of 2021
Dec 22, 2021
Here we present a small selection of 12 spectacular species that were newly discovered in 2021 with links to their complete taxonomic treatment. more
Annotating genes sequences with data from herbarium sheets and publications
Nov 11, 2021
A report on a workshop on updating accession with specimen-data from publications more

hi knowledge

dive into science

VISUALISATION TOOLS INFO & VISION FUNDING LINKS & PUBLICATIONS CONTACT

Interactive visualisation tools for a better understanding of science and nature

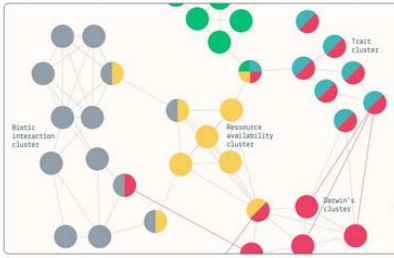

Invasion biology:

large hypothesis network

Interactive network showing clusters of 39 invasion hypotheses, based on Enders et al. (2020) and the book Invasion Biology: Hypotheses and Evidence (Jeschke & Heger, eds, 2018; CABI, Wallingford, UK). This tool is an extension of the smaller network with 12 hypotheses.

Launch visualisation

PLAZI

TREATMENTBANK BIODIVERSITY LITERATURE REPOSITORY SERVICES HOW TO PARTICIPATE ABOUT

Arcadia Fund supports Plazi in its endeavor to rediscover known biodiversity

May 16, 2022

Plazi will utilize a grant from Arcadia Fund to accelerate discovery of known biodiversity by expanding the existing corpus of the Biodiversity Literature Repository more

Access to taxonomic treatments mentioned in press releases

Jan 14, 2022

Result of an experiment to test how easy it is to locate the original taxonomic treatments of species mentioned in press releases more

New Species of 2021

Dec 22, 2021

Here we present a small selection of 12 spectacular species that were newly discovered in 2021 with links to their complete taxonomic treatment. more

Annotating genes sequences with data from herbarium sheets and publications

Nov 11, 2021

A report on a workshop on updating accession with specimen-data from publications more

STATS

Articles: 56539
Treatments: 808577
Occurrences: 265911
Material Citations (MC): 1267991
Geo-referenced MC: 375379

EVENTS

TAGS

ABOUT (6) BICIKL (1) BLR (1) BLUE LIST (1) DAK (1) DATA, API AND TOOLS (13) DATA QUALITY (1) EVENTS (16) GOLDEN GATE (2) LECTURES (1) LEGAL ISSUES (4) MEMBERS (1) NEWS (29) PARTNERS (1) PROJECTS (1) PUBLICATIONS (1) REPOS (1) SERVICES (1) SOURCE CODE (1) TREATMENT BANK (10)

SOCIAL

Twitter
GitHub
info@plazi.org
Vimeo

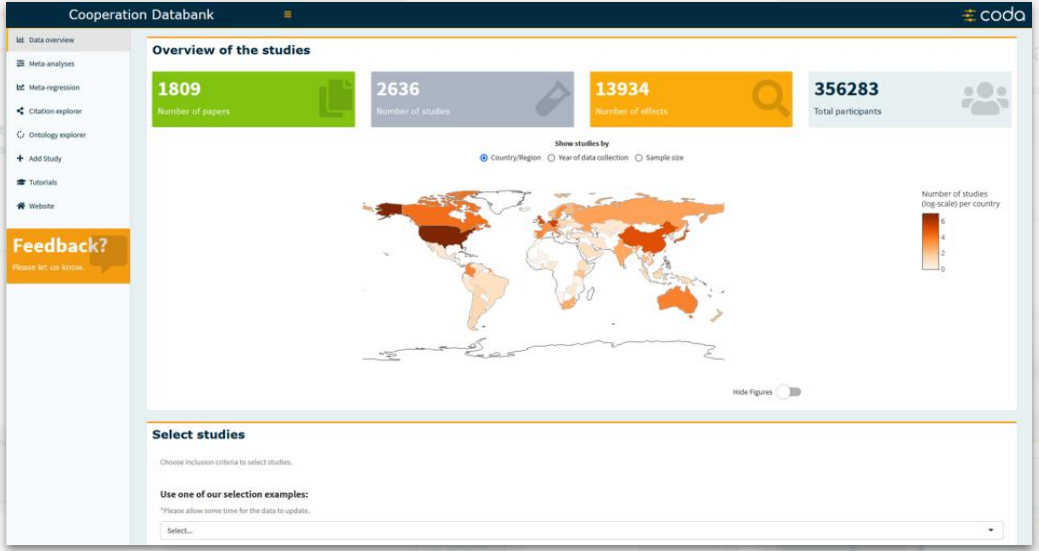
Cooperation Databank
coda
Data overview
Meta-analyses
Meta-regression
Citation explorer
Ontology explorer
Add Study
Tutorials
Website
Feedback?
Please let us know.
Overview of the studies
1809
Number of papers
2636
Number of studies
13934
Number of effects
356283
Total participants
Show studies by
Country/Region
Year of data collection
Sample size
Number of studies (log-scale) per country
Hide Figures
Select studies
Choose inclusion criteria to select studies.
Use one of our selection examples:
*Please allow some time for the data to update.
Select...

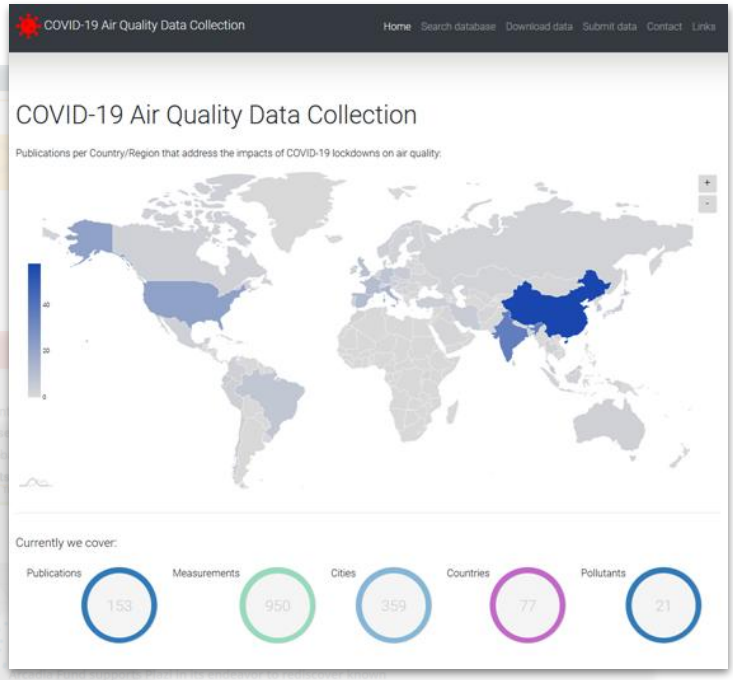
COVID-19 Air Quality Data Collection
Home
Search database
Download data
Submit data
Contact
Links
COVID-19 Air Quality Data Collection
Publications per Country/Region that address the impacts of COVID-19 lockdowns on air quality:
Currently we cover:
Publications
153
Measurements
950
Cities
359
Countries
77
Pollutants
21

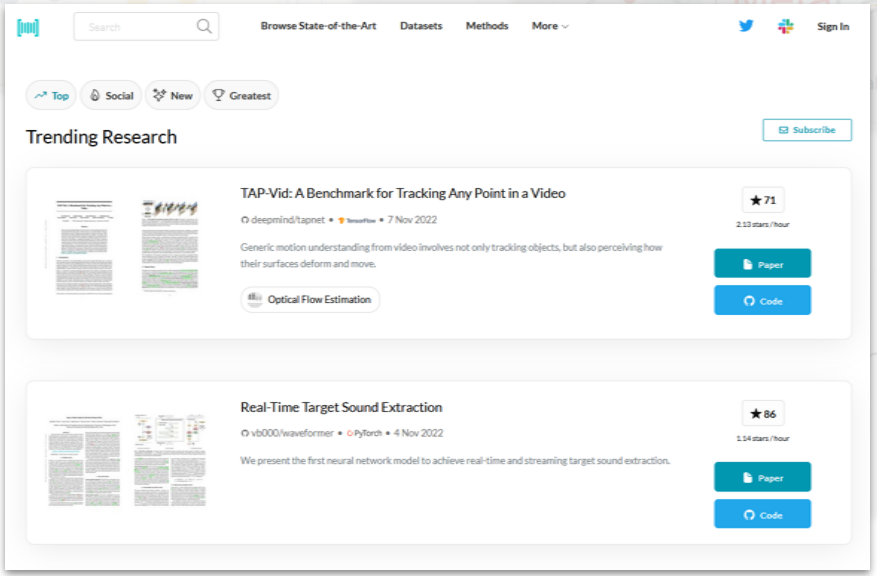
Search
Browse State-of-the-Art
Datasets
Methods
More
Sign In
Top
Social
New
Greatest
Trending Research
Subscribe
TAP-Vid: A Benchmark for Tracking Any Point in a Video
deepmind/tapnet • TensorFlow • 7 Nov 2022
Generic motion understanding from video involves not only tracking objects, but also perceiving how their surfaces deform and move.
Optical Flow Estimation
★ 71
2.13 stars / hour
Paper
Code
Real-Time Target Sound Extraction
vb000/waveformer • PyTorch • 4 Nov 2022
We present the first neural network model to achieve real-time and streaming target sound extraction.
★ 86
1.14 stars / hour
Paper
Code

MetaLab Explore Data Documentation Publications Team

MetaLab

Interactive, community-augmented meta-analysis tools for cognitive development research

The MetaLab database contains **2,497 effect sizes** from **30 meta-analyses** across two domains of cognitive development, based on data from **688 papers** and **45,260 subjects**.

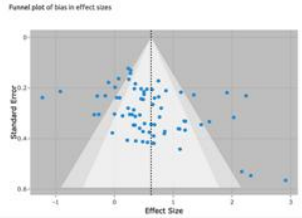

New: The 2020 Contribution Challenge Winners

Explore Apps View Documentation ›

New MetaLab User? Check out Getting Started first!

Domains

Early Language

How do children learn their native language?

Cognitive Development

What is the nature of children's understanding?

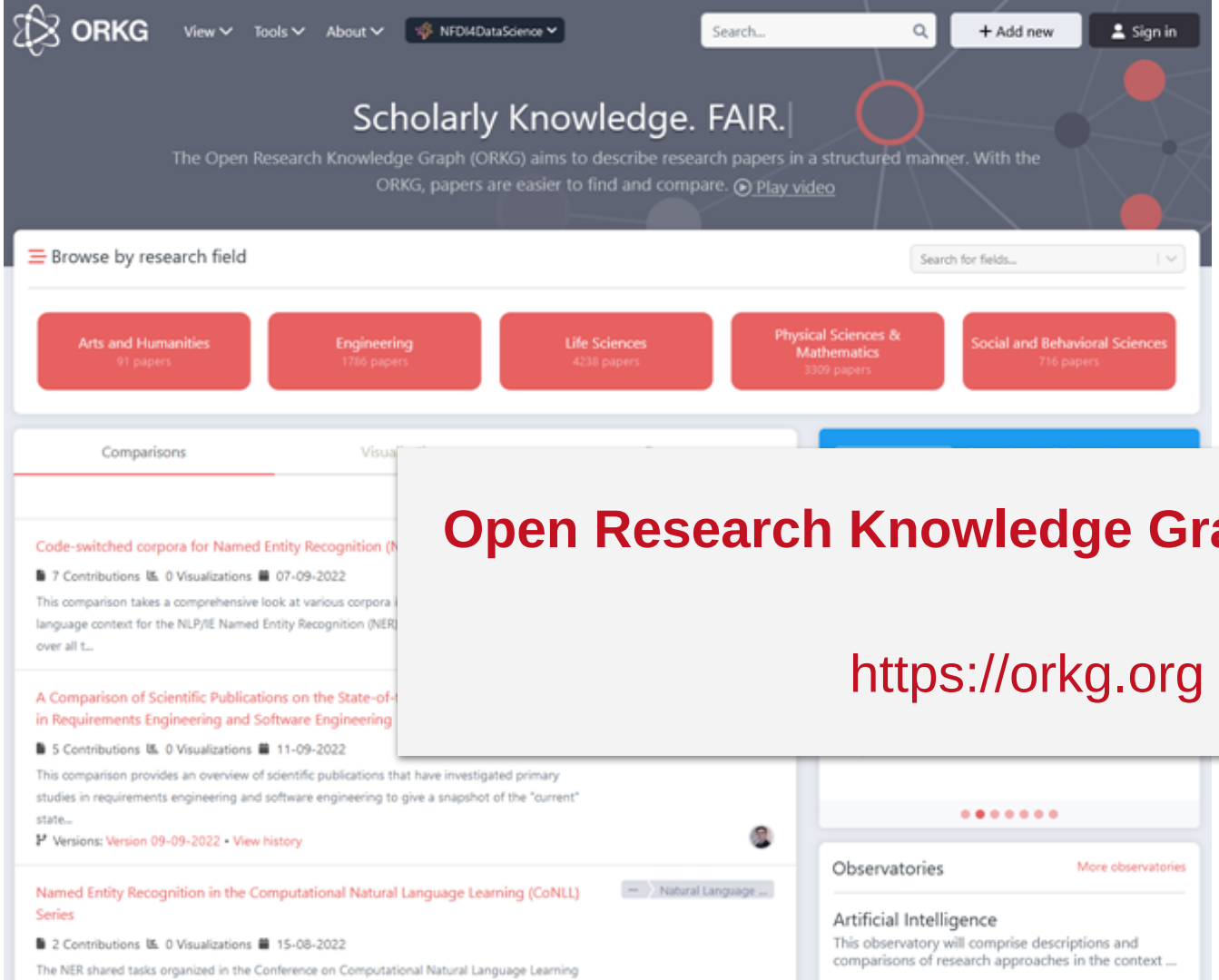

Open Research Knowledge Graph

https://orkg.org • @orkg_org

The benefits are obvious

Properties	The early phase of the COVID-19 outbreak in Lombardy, Italy *2020 - Contribution 1*	Transmission potential of COVID-19 in Iran *2020 - Contribution 1*	Transmission potential of COVID-19 in Iran *2020 - Contribution 2*	Estimating the generation interval for COVID-19 based on symptom onset data *2020 - Contribution 1*
location	Lombardy, Italy	Iran	Iran	Singapore
Time period	Time interval	Time interval	Time interval	Time interval
has beginning	2020-01-14	2020-02-19	2020-02-19	2020-01-21
has end	2020-03-08	2020-02-29	2020-02-29	2020-02-26
Basic reproduction number	Basic reproduction number estimate value specification	Basic reproduction number estimate value specification	Basic reproduction number estimate value specification	Basic reproduction number estimate value specification
Has value	3.1	3.6	3.58	1.27
Confidence interval (95%)	Confidence interval (95%)	Confidence interval (95%)	Confidence interval (95%)	Confidence interval (95%)
Lower confidence limit	2.9	3.4	1.29	1.19
Upper confidence limit	3.2	4.2	8.46	1.36

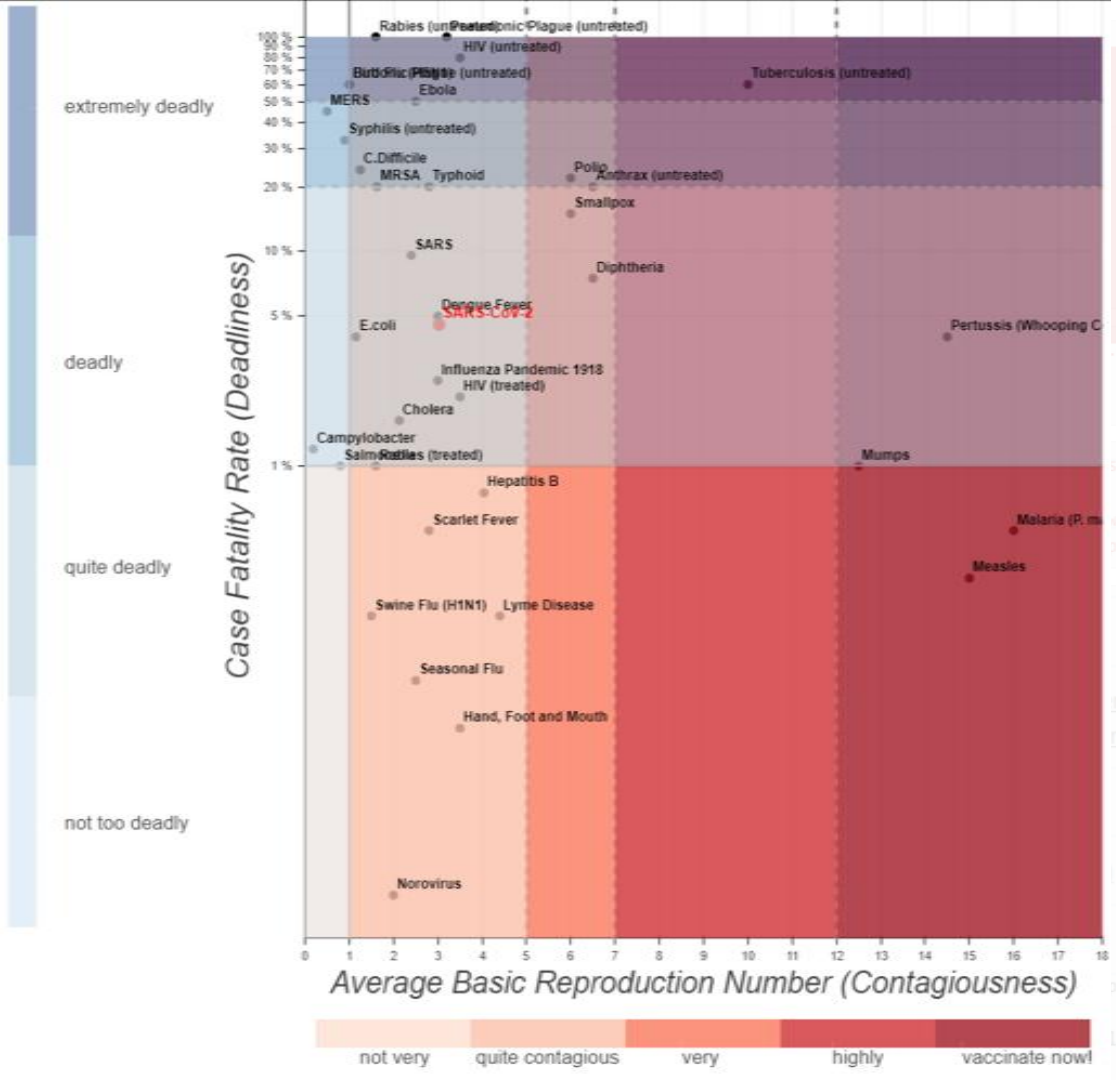

Transmission potential of COVID-19 in Iran

2020 - Contribution 2

Estimating the generation interval for COVID-19 based on symptom onset data

2020 - Contribution 1

ResetTool, SaveTool, PanTool, DatetimeTickFormatter, Whisker

.org/orkg/simcomp')

Iran

Singapore

s end', :]])

Time interval

Time interval

er confidence limit', :]])

er confidence limit', :]])

2020-02-19

2020-01-21

2020-02-29

2020-02-26

Basic reproduction number estimate value specification

Basic reproduction number estimate value specification

3.58

1.27

Confidence interval (95%)

Confidence interval (95%)

1.29

1.19

pper=upper))

8.46

1.36

lot_height=350, tools=[hover1, WheelZoomTool(), PanTool(), ResetTool(),

```
[ ]: import requests
     import datetime
     import pandas as pd
     import numpy as np
     from orkg import ORKG
     from bokeh.io import export_png
     from bokeh.models import ColumnDataSource, HoverTool, WheelZoomTool, ResetTool, SaveTool, PanTool, DatetimeTickFormatter, Whisker
     from bokeh.plotting import figure, show, output_notebook

     output_notebook()
```

```
[ ]: orkg = ORKG(host='https://orkg.org/orkg', simcomp_host='https://orkg.org/orkg/simcomp')

     df = orkg.contributions.compare_dataframe(comparison_id='R44930')
```

```
[ ]: dates = np.array([datetime.date.fromisoformat(x) for x in df.loc['has end', :]])
     values = np.float32(df.loc['Has value', :])
     lower = np.array([np.float32(x) if x else np.nan for x in df.loc['Lower confidence limit', :]])
     upper = np.array([np.float32(x) if x else np.nan for x in df.loc['Upper confidence limit', :]])
```

```
[ ]: hover1 = HoverTool(
         tooltips=[
             ('Date', '@date{%F}'),
             ('R0', '@value{0.ff}'),
             ('95% CI', '@lower{0.ff}-@upper{0.ff}')
         ],
         formatters={
             '@date': 'datetime',
             '@{value}' : 'printf',
             '@{lower}' : 'printf',
             '@{upper}' : 'printf'
         }
     )

     df = pd.DataFrame(data=dict(date=dates, value=values, lower=lower, upper=upper))
     source = ColumnDataSource(df)
     p = figure(x_axis_type="datetime", y_range=(0, 9), plot_width=800, plot_height=350, tools=[hover1, WheelZoomTool(), PanTool(), ResetTool(),
     p.xaxis.formatter=DatetimeTickFormatter(days=['%d %b'])
```

DataCite Commons

10.48366/r44930

Pages Support Sign In

Works People Organizations Repositories

1 Work

Publication Year

- [ ] 2020 1

Work Type

- [ ] Dataset 1

License

- [ ] CC-BY-SA-4.0 1

COVID-19 Reproductive Number Estimates

Allard Oelen, Jennifer D'Souza, Markus Stocker, Lars Vogt, Kheir Eddine Farfar, Muhammad Haris, Kamel Fadel, Mohamad Yaser Jaradeh & Vitalis Wiens

Comparison published 2020 in Open Research Knowledge Graph (ORKG)

Comparison of published reproductive number estimates for the COVID-19 infectious disease

DOI registered October 16, 2020 via DataCite.

Dataset English

https://doi.org/10.48366/r44930

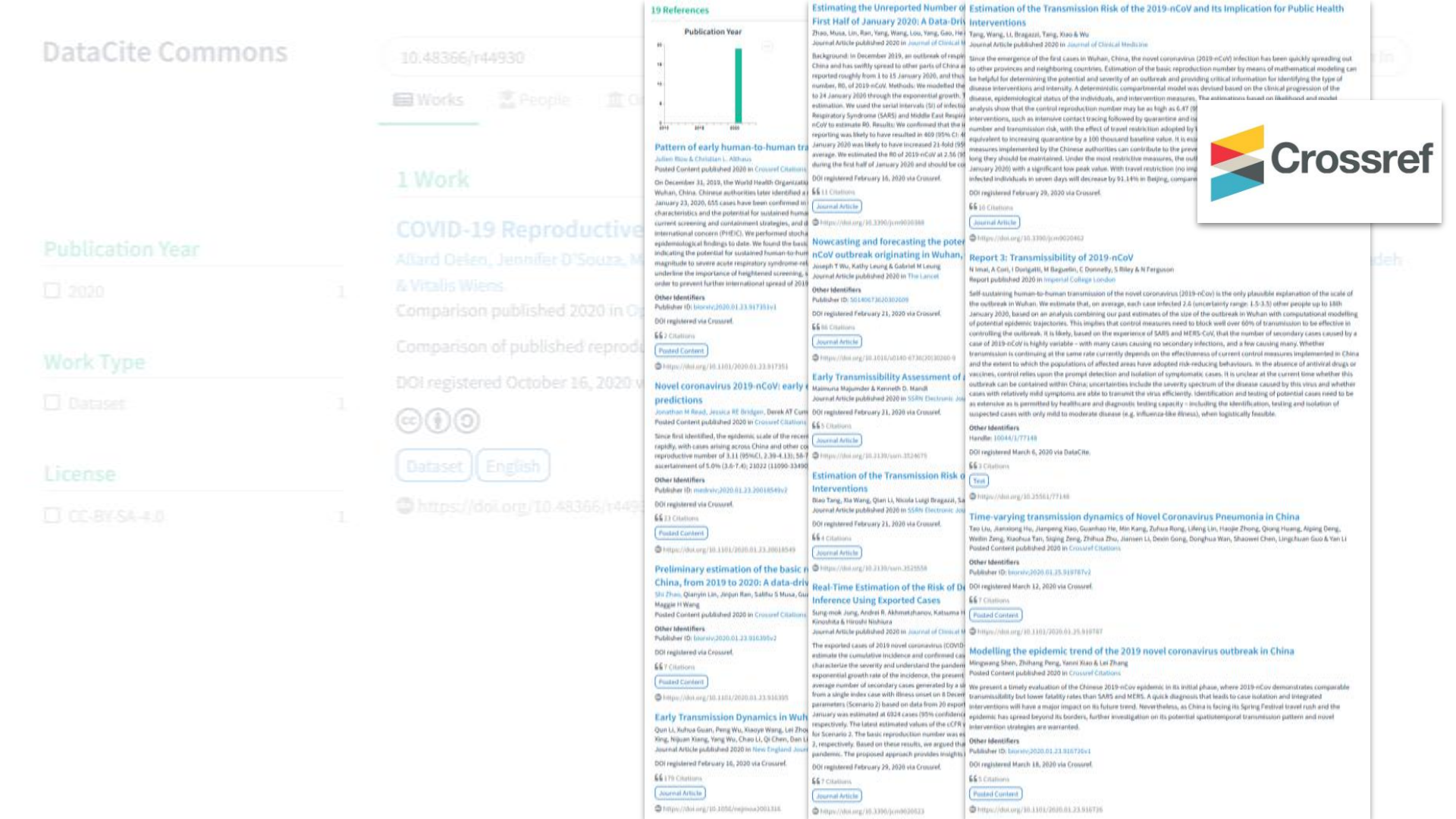
19 References
Publication Year
Pattern of early human-to-human tra
Novel coronavirus 2019-nCoV: early
predictions
Preliminary estimation of the basic
China, from 2019 to 2020: A data-driv
Early Transmission Dynamics in Wuh
Estimating the Unreported Number o
First Half of January 2020: A Data-Dri
Nowcasting and forecasting the pote
nCoV outbreak originating in Wuhan,
Early Transmissibility Assessment of
Estimation of the Transmission Risk o
Interventions
Real-Time Estimation of the Risk of D
Inference Using Exported Cases
Estimation of the Transmission Risk of the 2019-nCoV and Its Implication for Public Health
Interventions
Report 3: Transmissibility of 2019-nCoV
Time-varying transmission dynamics of Novel Coronavirus Pneumonia in China
Modelling the epidemic trend of the 2019 novel coronavirus outbreak in China
Crossref

DataCite Commons

Type to search...

Pages Support Sign In

Works People Organizations Repositories

https://doi.org/10.1101/2020.03.08.20030643

Transmission potential of COVID-19 in Iran

Kamalich Muniz-Rodriguez, Isaac Chun-Hai Fung, Shayesterh R. Ferdosi, Sylvia K. Ofori, Yiseul Lee, Amna Tariq & Gerardo Chowell

Posted Content published 2020 via medRxiv

We computed reproduction number of COVID-19 epidemic in Iran using two different methods. We estimated R0 at 3.6 (95% CI, 3.2, 4.2) (generalized growth model) and at 3.58 (95% CI, 1.29, 8.46) (estimated epidemic doubling time of 1.20 (95% CI, 1.05, 1.44) days) respectively. Immediate social distancing measures are recommended.

Other Identifiers

Publisher ID: medrxiv;2020.03.08.20030643v1

DOI registered April 10, 2020 via Crossref.

2 Citations

Posted Content

https://doi.org/10.1101/2020.03.08.20030643

2 Citations

COVID-19 Reproductive Number Estimates

Allard Oelen, Jennifer D'Souza, Markus Stocker, Lars Vogt, Kheir Eddine Farfar, Muhammad Haris, Kamel Fadel, Mohamad Yaser Jaradeh & Vitalis Wiens

Comparison published 2020 in Open Research Knowledge Graph (ORKG)

Comparison of published reproductive number estimates for the COVID-19 infectious disease

DOI registered October 16, 2020 via DataCite.

Dataset English

https://doi.org/10.48366/r44930

Filter Works

Type to search...

Publication Year

2020 2

Work Type

Dataset 1

So why is most scientific information still buried in documents?

Because it is hard to produce FAIR scientific information

Post-publication / Manually

Basic reproduction number	3.1
location	Lombardy, Italy
Time period	2020-01-14 - 2020-03-08
research problem	Determination of the COVID-19

Cancel Create

Determination of the COVID-19 basic reproduction number
→ *Referred: 35 times* Instance of: *Problem*
ORKG

+ Add property

Post-publication / Automatically

The suggestions listed below are automatically generated based on the title and abstract from the paper. Using these suggestions is optional.

tract

+ Suggestions

eferences

Statements

Research problem

- environmental phenomena
- monitoring of atmospheric phenomena
- organization and interpretation of sensor data
- scientific computing workflows

Resource

- Sensor Data

Pre-publication / FAIR at birth

Production

```
# Two Linear Mixed Model (LMM) computations
lm.mwd.1 <- lmer(MWD_cor ~ cc_variant + (1|depth), data = df.MWD)
lm.mwd.2 <- lmer(MWD_cor ~ cc_type + (1|depth), data = df.MWD)

# Output data for the two LMM
df1 <- data.frame(summary(lm.mwd.1)$coefficients, check.names=FALSE)
df2 <- data.frame(summary(lm.mwd.2)$coefficients, check.names=FALSE)

instance <- tp$model_fitting(
  label="Linear mixed model fitting with MWD as response, CC variant as predictor variable, and soil depth as random variable",
  has_input_dataset=tuple(df.MWD, "Difference of mean weight diameter between the dry and wet sieving method"),
  has_input_model=tp$statistical_model(
    label="A linear mixed model with MWD as response and CC variant as predictor variable",
    is_denoted_by=tp$formula(
      label="The formula of the linear mixed model with MWD as response and CC variant as predictor variable",
      has_value_specification=tp$value_specification(
        label="MWD_cor ~ cc_variant + (1|depth)",
        has_specified_value="MWD_cor ~ cc_variant + (1|depth)"
      )
    )
  ),
  has_output_dataset=tuple(df1, "Results of LMM with MWD as response and CC variant as predictor variable")
)
instance$serialize_to_file("article.contribution.1.json", format="json-ld")
```

Pre-publication / FAIR at birth

Publication

Copernicus Publications
The Innovative Open Access Publisher

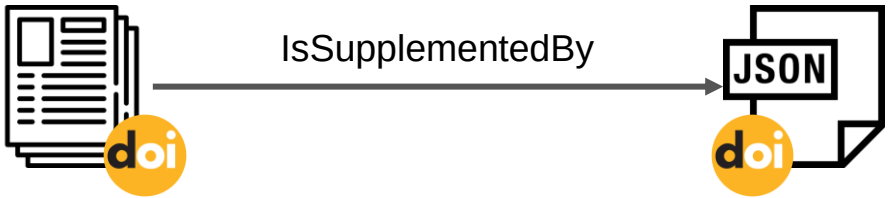

Pre-publication / FAIR at birth

Harvesting

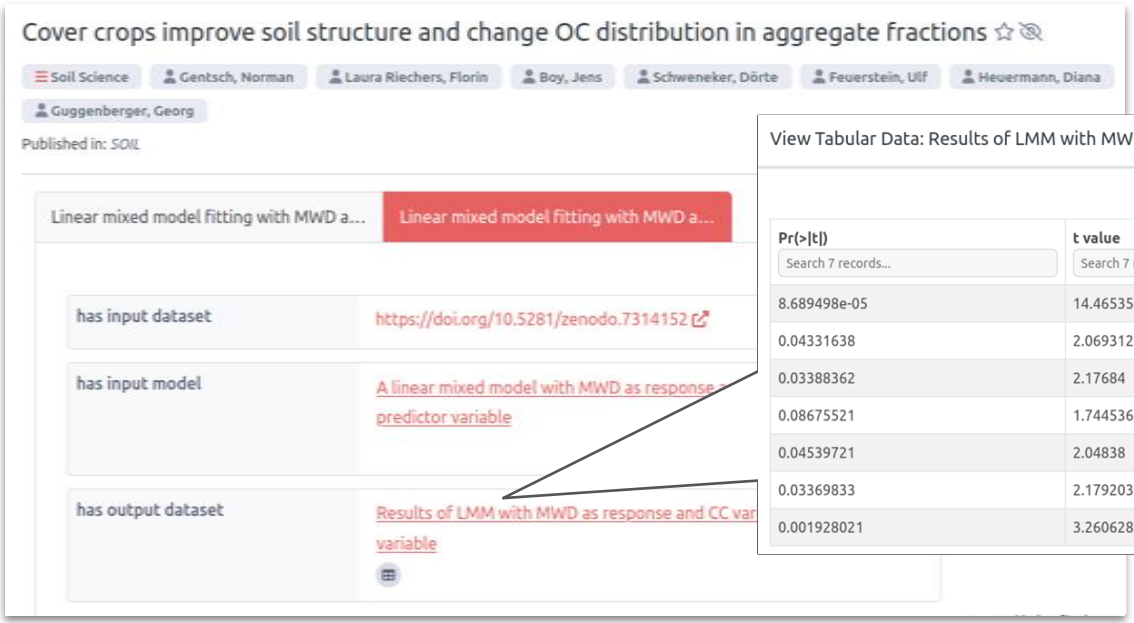

View Tabular Data: Results of LMM with MWD as response and CC variant as predictor variable

Pr(>|t|)	t value	df
Search 7 records...	Search 7 records...	Search 7 records...
8.689498e-05	14.46535	4.267258
0.04331638	2.069312	54.0
0.03388362	2.17684	54.0
0.08675521	1.744536	54.0
0.04539721	2.04838	54.0
0.03369833	2.179203	54.0
0.001928021	3.260628	54.0

FAIR scientific information. It’s time.